Volume 1 | Number 1 | Jan 2013 | Pages 1–100

ChemComm

Chemical Communications
www.rsc.org/chemcomm

ROYAL SOCIETY OF CHEMISTRY

This is an *Accepted Manuscript*, which has been through the Royal Society of Chemistry peer review process and has been accepted for publication.

Accepted Manuscripts are published online shortly after acceptance, before technical editing, formatting and proof reading. Using this free service, authors can make their results available to the community, in citable form, before we publish the edited article. We will replace this *Accepted Manuscript* with the edited and formatted *Advance Article* as soon as it is available.

You can find more information about *Accepted Manuscripts* in the **Information for Authors**.

Please note that technical editing may introduce minor changes to the text and/or graphics, which may alter content. The journal's standard **Terms & Conditions** and the **Ethical guidelines** still apply. In no event shall the Royal Society of Chemistry be held responsible for any errors or omissions in this *Accepted Manuscript* or any consequences arising from the use of any information it contains.

ROYAL SOCIETY OF CHEMISTRY

www.rsc.org/chemcomm

ARTICLE TYPE

g-C$_3$N$_4$ Quantum Dots: Direct Synthesis, Upconversion Property and Photocatalytic Application

**Wanjun Wang, Jimmy C. Yu**[*]**, Zhurui Shen, Ka Long Chan, Ting Gu**

Graphitic carbon nitride (g-C$_3$N$_4$) quantum dots (CNQDs) were prepared from bulk g-C$_3$N$_4$ directly by a thermal-chemical etching process. The CNQDs show strong blue emission as well as upconversion behavior, which can be used 10 as a universal energy-transfer component in visible-light-driven metal-free photocatalytic systems.

The development of highly efficient photocatalysts for solar energy conversion has attracted worldwide attention. For example, graphitic carbon nitride (g-C$_3$N$_4$) was found to be 15 effective for solar-induced H$_2$ evolution, CO$_2$ photofixation, and environmental purification.[1] This metal-free photocatalyst contains only carbon and nitrogen which are among the most abundant elements on our planet. However, currently available g-C$_3$N$_4$-based materials are generally sub-micrometer-sized 20 nanoplate, nanosphere, and nanorods.[2] As an analogue, graphene has been fabricated into narrow nanoribbons (GNRs) and quantum dots (GQDs) with sizes less than 10 nm.[3] The strong quantum confinement and edge effects when the sizes are down to 10 nm render graphene with excellent optical properties, which 25 has been used to design GQDs-based photocatalysts, such as GQD/TiO$_2$.[4] In this context, it would be interesting to develop effective routes for cutting bulk g-C$_3$N$_4$ into nanometer-sized pieces of well-confined shapes, such as g-C$_3$N$_4$ nanoribbons (CNNRs) and g-C$_3$N$_4$ quantum dots (CNQDs).

30 CNQDs can be synthesized from starting materials such as formamide and urea.[5] To the best of our knowledge, the preparation of CNNRs has never been reported. Herein, we describe a controllable process for directly cutting 3D bulk

g-C$_3$N$_4$ into 2D nanosheets, 1D CNNRs and finally to 0D CNQDs. As shown in Scheme 1, this process starts with the 50 exfoliation of bulk g-C$_3$N$_4$ into nanosheets. Different from graphite where there is weak van der Waals force between layers, the planar cohesion of the g-C$_3$N$_4$ is mainly contributed by hydrogen bonding between strands of polymeric melon units with NH/NH$_2$ groups,[6] thus the Hummers method which are widely 55 used for exfoliation of graphite into graphene is not suitable for making monolayer or a few layers of g-C$_3$N$_4$ nanosheets. Therefore, we employ a thermal oxidation method suggested by Liu et al. to etch bulk g- C$_3$N$_4$ to graphene-like nanosheets (Fig. 1b).[7] Then, the obtained
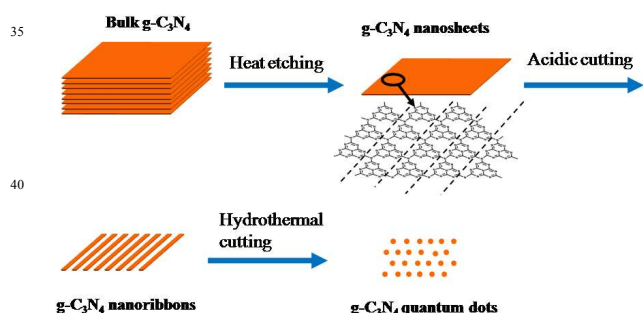
Scheme 1 Schematic illustration of the controllable synthesis of g-C$_3$N$_4$ nanosheets, nanoribbons and quantum dots
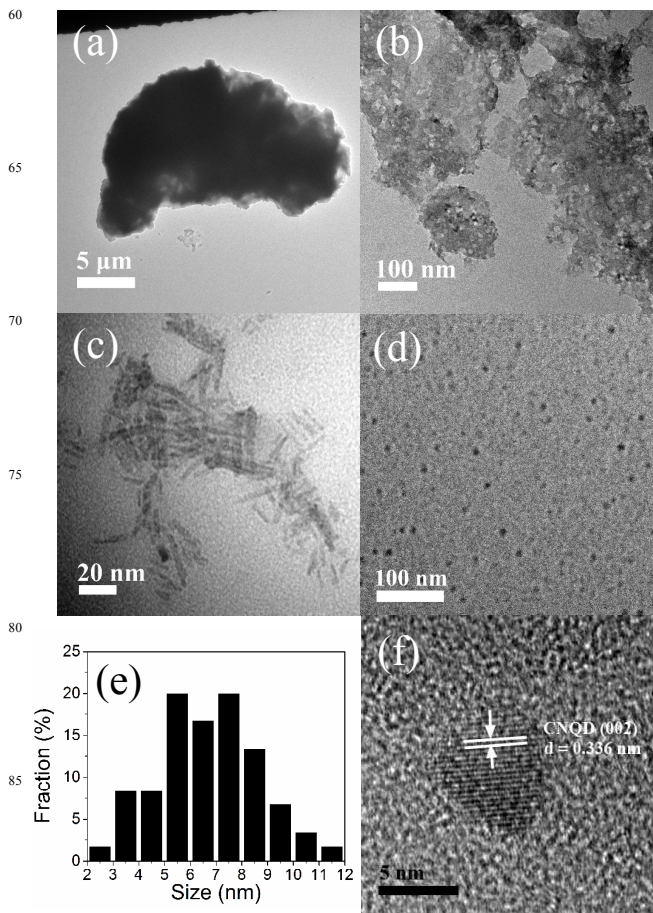
Fig. 1 TEM images of (a) bulk g-C$_3$N$_4$, (b) g-C$_3$N$_4$ nanosheets, (c) CNNRs and (d) CNQDs; (e) Diameter distribution of the CNQDs; (f) HRTEM of a single CNQD

g-C$_3$N$_4$ nanosheets are subjected to acidic etching by concentrated H$_2$SO$_4$ and HNO$_3$ to produce CNNRs. During this process, some C-N bonds which connect the tri-s-triazine units are oxidized and oxygen-containing functional groups, such as carboxylate groups, are introduced at the edge and on the basal plane, as shown in the FT-IR spectrum (Fig. S1). This leads to orientational cleavage of g-C$_3$N$_4$ nanosheets to CNNRs with particle sizes less than 10 nm in width and several tens of nm in length (Fig. 1c).

Finally, CNQDs are obtained after the hydrothermal treatment of CNNRs at 200 °C (pH = 5). The detailed experimental procedure can be found in the supporting information. Typical TEM image shows that the diameters of as-prepared CNQDs are in the range of 5 - 9 nm (6.7 nm average diameter) (Fig. 1d and e). The lattice spacing of CNQDs is 0.336 nm (Fig. 1f), corresponding to the (002) plane of hexagonal g-C$_3$N$_4$ (JCPDS 87-1526).[8] The formation of hydrophilic carboxylate groups by hydrothermal treatment of CNNRs (Fig. S1) makes CNQDs highly soluble in water. The CNQDs solution is stable in ambient condition for at least 8 months. High-resolution XPS spectra of C1s and N1s reveal that triazine units remain in the CNQDs with surface amino-functional and carbonyl-functional groups (Fig. S2). The total N content reaches as high as 19.94%, which exceeds the reported N-doped carbon/graphene quantum dots,[9] because the high N content is intrinsically from bulk g-C$_3$N$_4$ instead of external doping. Other N-containing byproducts may also exist on the CNQDs which needs further investigation.

The as-synthesized CNQDs emit bright blue luminescence under UV excitation, which may show promising applications in bioimaging and biolabelling (Fig. 2a). In addition, it shows excitation wavelength-dependent PL spectra. When the excitation wavelength is varied from 340 to 420 nm, the PL peak shifts to longer wavelengths. Moreover, the emission intensity increases slightly first and then decreases rapidly, with the strongest peak appears upon 360 nm excitation. If the hydrothermal temperature is decreased to 180 °C, the PL intensity would also decrease significantly (Fig. S3a). The intrinsic luminescence mechanism of CNQDs may be ascribed to the $\pi - \pi^*$ transition in the aromatic structure.[10]

Interestingly, the CNQDs were found to exhibit obvious upconversion property when excited by long-wavelength light. As shown in Fig. 2b, irradiating CNQDs with 705 to 862 nm light

would generate emissions in the range of 350 to 600 nm. This covers a wide spectrum of the visible-light region. The upconversion PL excitation (PLE) spectrum recorded with the strongest luminescence at 440 nm shows several overlapped peaks centered at 705, 725, 750 and 778 nm (Fig. S3b), which should be associated with corresponding absorption bands. There are two kinds of popular mechanisms for the upconversion emission: the multiphoton active process and anti-Stokes photoluminescence.[11] Considering that the energy difference between the excitation light and the emission light in the upconversion process is not a fixed value, the multiphoton active process is probably more suitable for explaining the upconversion emission of CNQDs

The above results confirm that the CNQDs can convert NIR light to visible light. This makes the material useful as a universal energy-transfer component in a photocatalytic system. Solar energy harvesting can be enhanced due to the utilization of the NIR region. To demonstrate this possibility, we added the CNQDs solution on bulk g-C$_3$N$_4$ to construct a metal-free isotype heterojunction. It should be noted that the development of metal-free photocatalysts has become an intensively perused topic in view of the concept of "green photocatalysis".[12] The CNQDs/g-C$_3$N$_4$ suspension was used for H$_2$ evolution from water splitting in the presence of 1 wt% Pt as a co-catalyst and 10% triethanolamine as a sacrificial agent. Fig. 3a shows the formation of H$_2$ at rates of 48.05 and 109.96 μmol/h for bulk g-C$_3$N$_4$ and CNQDs/g-C$_3$N$_4$ (5 mL CNQD addition; Sample CN-5). Further increasing the amount of CNQDs to 10 mL, the H$_2$ production efficiency reached 137.84 μmol/h (Sample CN-10). No pH change was observed before and after adding 5 or 10 mL CNQDs in this system (pH = 11.12). Therefore, the use of CNQDs as an energy-transfer component can effectively enhance the visible-light-driven photocatalytic activity by at least 2.87 times. The TEM images of CN-10 loading with Pt after the H$_2$ evolution experiments show that CNQDs and Pt nanoparticle clusters are anchored on the surface of bulk g-C$_3$N$_4$ (Fig. S4). The loading of
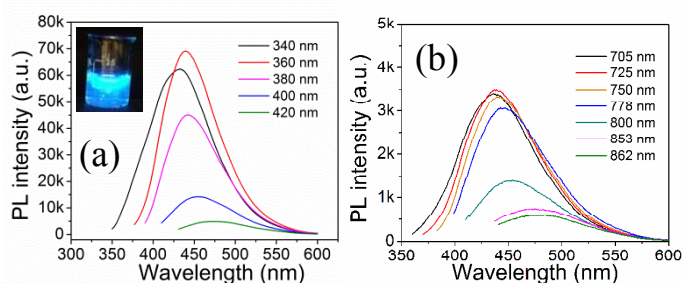

Fig. 2 (a) PL spectra of the CNQDs at different excitation wavelengths. Inset: Photograph of the CNQDs aqueous solution taken under 365 nm UV light. (b) The upconversion PL spectra of the CNQDs.
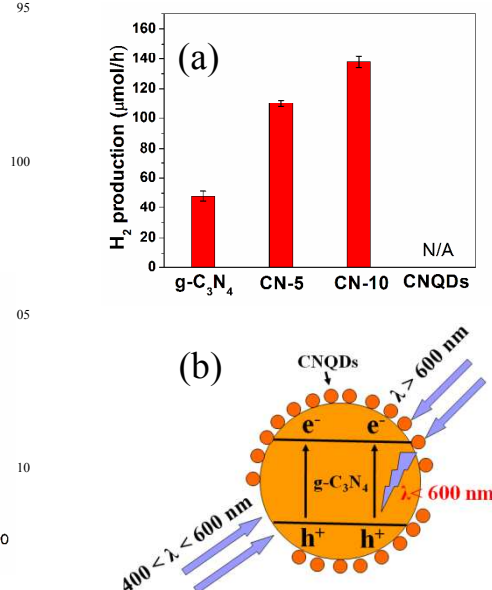

Fig. 3 (a) Photocatalytic H$_2$ production for the samples with 1 wt% Pt under visible light irradiation (λ > 420 nm) using triethanolamine as the

sacrificial agent. (b) Proposed photocatalytic mechanism for CNQDs/g-C_3N_4 under visible light.

Pt violates the "metal-free" principle, thus the activities of g-C_3N_4 and CN-10 were also studied without Pt loading. Results show that the H_2 production rate by g-C_3N_4 is decreased to 8.17 μmol/h, while the rate by CN-10 is decreased to 18.58 μmol/h, which is still about 2.27 times than the bare g-C_3N_4 (Fig. S5). In contrast, no H_2 evolution is observed when using pure CNQDs (10 mL) as the photocatalyst, which indicates that CNQDs has no intrinsic activity but play a crucial role in accelerating photocatalytic reactions.

As mentioned above, the pH effect is negligible, and there is no obvious change in surface area before and after CNQDs modification. The possible mechanism is shown in Fig. 3b which suggests the utilization of both short and long wavelengths in the spectrum. Upon photo-excitation, visible light with wavelength shorter than 600 nm can directly excite the as-prepared g-C_3N_4.[13] Meanwhile, the long wavelength (λ > 600 nm) is upconverted by CNQDs for the subsequent excitation of g-C_3N_4 to form electron-hole pairs. The UV-vis absorption of the samples shows that the long wavelength (λ > 600 nm) absorption is enhanced by modification with CNQDs (Fig. S6). In addition, we also conducted hydrogen evolution experiments under long wavelengths using a 600 nm cut-off filter. As shown in Fig. S7, no hydrogen were detected on g-C_3N_4, while 10.91 and 18.92 μmol/h were detected on sample CN-5 and CN-10, respectively. These results further support the mechanism that the g-C_3N_4/CNQDs can utilize long wavelength by taking advantage of the upconversion property of CNQDs. Moreover, the isotype heterojunctions allows fast charge transfer across the interfaces for this metal-free photocatalyst.[14] For comparison, CNQDs were also added to the well-known P25 (TiO$_2$), as a portion of the upconversion emission (350-550 nm) is located in the UV region (λ < 380 nm). Results show that the H_2 production rate of P25 could be enhanced by 51.8 times under visible light irradiation (Fig. 4).
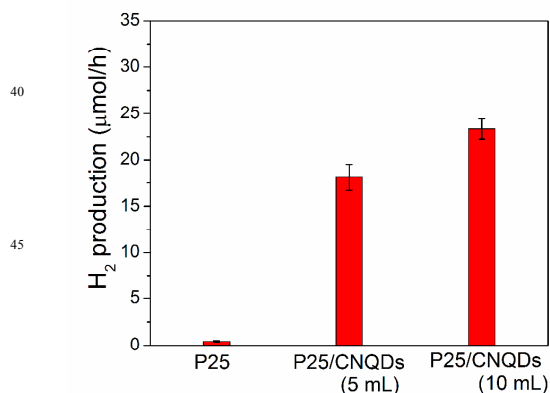

Fig. 4 Photocatalytic H_2 production for the samples with 1 wt% Pt under visible light irradiation (λ > 420 nm) using 10% methanol as the sacrificial agent.

In summary, we presented here a controllable method for cutting bulk g-C_3N_4 to nanosheets, nanoribbons and quantum dots. The upconversion behavior of as-prepared CNQDs was found for the first time. As a result, CNQDs shows promise to be used as a general energy-transfer component in photocatalytic systems to harness the Vis-NIR spectrum of sunlight.

Notes and references

Department of Chemistry, Shenzhen Research Institute and Institute of Environment, Energy and Sustainability, The Chinese University of Hong Kong, Shatin, N.T., Hong Kong, CHINA
E-mail: jimyu@cuhk.edu.hk (J.C. Yu)

† Electronic Supplementary Information (ESI) available: Details of sample preparation, characterization, experimental condition for H_2 evolution, FI-IR spectra, High resolution XPS spectra and PL spectra. See DOI: 10.1039/b000000x/

1 (a) X. C. Wang, K. Maeda, A. Thomas, K. Takanabe, G. Xin, J. M. Carlsson, K. Domen and M. Antonietti, *Nat. Mater.*, 2009, **8**, 76-80. (b) G. Liu, P. Niu, C. H. Sun, S. C. Smith, Z. G. Chen, G. Q. Lu and H. M. Cheng, *J. Am. Chem. Soc.*, 2010, **132**, 1642-11648. (c) D. H. Wang, Y. W. Zhang and W. Chen, *Chem. Commun.*, 2014, **50**, 1754-1756. (d) J. H. Li, B. A. Shen, Z. H. Hong, B. Z. Lin, B. F. Gao and Y. L. Chen, *Chem. Commun.*, 2012, **48**, 12017-12019. (e) Y. D. Hou, A. B. Laursen, J. S. Zhang, G. G. Zhang, Y. S. Zhu, X. C. Wang, S. Dahl and I. Chorkendorff, *Angew. Chem. Int. Edit.*, 2013, **52**, 3621-2625. (f) J. S. Zhang, M. W. Zhang, G. G. Zhang and X. C. Wang, *ACS Catal.*, 2012, **2**, 940-948.
2 (a) J. L. Zimmerman, R. Williams, V. N. Khabashesku and J. L. Margrave, *Nano Lett.*, 2001, **1**, 731-734. (b) X. J. Bai, L. Wang, R. L. Zong and Y. F. Zhu, *J. Phys. Chem. C*, 2013, **117**, 9952-9961.
3 (a) X. Li, X. Wang, L. Zhang, S. Lee and H. Dai, *Science*, 2008, **319**, 1229-1232. (b) L. A. Ponomarenko, F. Schedin, M. I. Katsnelson, R. Yang, E. W. Hill, K. S. Novoselov and A. K. Geim, *Science*, 2008, **320**, 356-358. (c) E. Lee, J. Ryu and J. Jang, *Chem. Commun.*, 2013, **49**, 9995-9997.
4 (a) S. J. Zhuo, M. W. Shao and S. T. Lee, *ACS Nano*, 2012, **6**, 1059-1064. (b) D. Y. Pan, C. Xi, Z. Li, L. Wang, Z. W. Chen, B. Luc and M. H. Wu, *J. Mater. Chem. A*, 2013, **1**, 3551-3555.
5 (a) S. Barman and M. Sadhukhan, *J. Mater. Chem.*. 2012, **22**, 21832-21837. (b) J. Zhou, Y. Yang and C. Y. Zhang, *Chem. Commun.*, 2013, **49**, 8605-8607.
6 B. V. Lotsch, M. Doblinger, J. Sehnert, L. Seyfarth, J. Senker, O. Oeckler and W. Schnick, *Chem. Eur. J.*, 2007, **13**, 4969-4980.
7 (a) P. Niu, L. L. Zhang, G. Liu and H. M. Cheng, *Adv. Funct. Mater.*, 2012, **22**, 4763-4770. (b) W. J. Wang, J. C. Yu, D. H. Xia, P. K. Wong and Y. C. Li, *Environ. Sci. Technol.*, 2013, **47**, 8724-8732.
8 (a) L. Ge, F. Zuo, J. K. Liu, Q. Ma, C. Wang, D. Z. Sun, L. Bartels and P. Y. Feng, *J. Phys. Chem. C*, 2012, **116**, 13708-13714. (b) L. Ge, C. C. Han, J. Liu and Y. F. Li, *Appl. Catal. A: Gen.*, 2011, **409–410**, 215-222.
9 (a) C. F. Wang, X. Wu, X. P. Li, W. T. Wang, L. Z. Wang, M. Gu and Q. Li, *J. Mater. Chem.*, 2012, **22**, 15522-15525. (b) Y. Q. Zhang, D. K. Ma, Y. Zhuang, X. Zhang, W. Chen, L. L. Hong, Q. X. Yan, K. Yu and S. M. Huang, *J. Mater. Chem.*, 2012, **22**, 16714-16718.
10 (a) V. N. Mochalin and Y. Gogotsi, *J. Am. Chem. Soc.*, 2009, **131**, 4594-4595. (b) D. Y. Pan, J. C. Zhang, Z. Li and M. H. Wu, *Adv. Mater.*, 2010, **22**, 734-738. (c) M. J. Krysmann, A. Kelarakis, P. Dallas and E. P. Giannelis, *J. Am. Chem. Soc.*, 2012, **134**, 7344-7350.
11 (a) L. Cao, X. Wang, M. J. Meziani, F. S. Lu, H. F. Wang, P. J. G. Luo, Y. Lin, B. A. Harruff, L. M. Veca, D. Murray, S. Y. Xie and Y. P. Sun, *J. Am. Chem. Soc.*, 2007, **129**, 11318-11319. (b) J. H. Shen, Y. H. Zhu, C. Chen, X. L. Yang and C. Z. Li, *Chem. Commun.*, 2011, **47**, 2580.
12 (a) G. Liu, P. Niu, L. C. Yin and H. M. Cheng, *J. Am. Chem. Soc.*, 2012, **134**, 9070-9073. (b) F. Wang, W. K. H. Ng, J. C. Yu, H. J. Zhu, C. H. Li, L. Zhang, Z. F. Liu and Q. Li, *Appl. Catal. B: Environ.*, 2012, **111-112**, 409-414. (c) G. Liu, P. Niu and H. M. Cheng, *ChemPhysChem*, 2013, **14**, 885-892.
13 G. G. Zhang, J. S. Zhang, M. W. Zhang and X. C. Wang, *J. Mater. Chem.*, 2012, **22**, 8083-8091.

ChemComm Accepted Manuscript

14   J. S. Zhang, M. W. Zhang, R. Q. Sun and X. C. Wang, *Angew. Chem. Int. Edit.*, 2012, **51**, 10145-10149.